Use of Multisine Signals For Efficient Behavioural Modelling of RF Circuits with Short-Memory Effects[1]

Dominique Schreurs and Kate A. Remley*

K.U.Leuven, Div. ESAT-TELEMIC, Kasteelpark Arenberg 10, B-3001 Leuven, Belgium
E-mail: Dominique.Schreurs@esat.kuleuven.ac.be
*National Institute of Standards and Technology, 325 Broadway, Boulder, CO 80305, USA

Abstract – *Behavioural models for RF devices are often based on single-tone data. However, this type of excitation is not representative of the digital modulation to which many RF devices are subjected in telecommunication systems. In this work, we show that the use of multisine excitation renders the modelling more efficient from both the experiment design and the data handling points of view, without loss of accuracy.*

I. Introduction

Large-signal models for RF devices are based usually on electrical equivalent-circuit schemes. This works fine as long as the devices are relatively simple (e.g., transistors) such that this circuit can be drawn based on pre-knowledge of the device's physical structure. A recent trend involves modelling not only on the component level, but also on the circuit level. By having one model for the circuit, instead of having a circuit design composed of several models for all the constitutive components, the required simulation time for a system design can be reduced significantly. However, such models can no longer be based on equivalent-circuit schemes, as the dynamics become complicated. Therefore, behavioural models are gradually being introduced to represent the characteristics of RF circuits. Most approaches reported in the literature make use of Volterra-series methods, which are restricted to weak non-linearities, and/or to band-limited models [1-3]. We adopted a state-space modelling approach that can handle strong non-linearities and that incorporates the modelling at the RF harmonics as well. This method has been introduced and described in detail in an earlier publication [4]. Its main principles will be reviewed in Section II. The results of [4] were, however, obtained from single-tone excitations, and from 2- or 3-tone experiments with a large-frequency offset between the tones (> 600 MHz). Those artificially chosen excitations are not realistic with respect to the actual use of RF circuits. RF circuits are embedded in telecommunication systems and, as such, subjected to (digitally) modulated excitations, with typical frequency offsets in the kHz range. The specific contribution of this paper is to investigate how our behavioural modelling approach can benefit from multisine excitations used to better approximate digital modulation [5].

II. RF Behavioural Modelling Approach

In case of a two-port RF device, we can rewrite the state equations describing the device's behaviour as follows:

[1] *Work partially supported by an agency of the U.S. government.*

0-7803-7143-7/02/$10.00 ©20023 IEEE.

$$I_1(t) = f_1\left(V_1(t), V_2(t), \dot{V}_1(t), \dot{V}_2(t), \ddot{V}_1(t), \cdots, \dot{I}_1(t), \dot{I}_2(t)\right) \quad (1)$$

and

$$I_2(t) = f_2\left(V_1(t), V_2(t), \dot{V}_1(t), \dot{V}_2(t), \ddot{V}_1(t), \cdots, \dot{I}_1(t), \dot{I}_2(t)\right) \quad (2)$$

with $I_i(t)$ the terminal currents, and $V_i(t)$ the terminal voltages. The superscript dots denote (higher-order) time derivatives. Note that the term 'RF device' encompasses not only simple RF components, such as transistors, but also RF circuits and even RF systems. We also could have expressed the terminal voltages as a function of the appropriate independent variables, but for the RF devices considered it is more straightforward to take the terminal currents as the dependent variables. An alternative however could be to express the scattered travelling voltage waves, b_1 and b_2, as functions of the incident waves a_1 and a_2 and the necessary derived state variables (such as the time derivatives of a_1 and a_2).

Note that equations (1) and (2) are applicable only to devices that exhibit no long-memory effects. In RF electronics, we typically distinguish between long and short memory effects. Short memory effects have time constants in the nanosecond range, on the order of the carrier-frequency period, while long memory effects have time constants in the millisecond or microsecond range, on the order of the IF-frequency period. Physical phenomena giving cause to the latter are traps and temperature effects. In the used formalism, it would mean that the terminal current at some time point t_{if} is also dependent on the terminal current value at previous IF sampling points. This extension of the formalism used is beyond the scope of this paper. The (higher-order) time derivatives in equations (1) and (2) ensure that short memory effects can be dealt with properly.

The purpose of the modelling approach is to determine the number of required state variables, and subsequently to determine the functions $f_1(.)$ and $f_2(.)$. The former can be accomplished by techniques based on the false-nearest-neighbour approach [6]. The latter is a function-fitting problem, by which an analytical formulation is selected; e.g., artificial neural networks, whose model parameters are determined by optimisation.

Typically, the available data for the modelling process are the time-domain terminal voltages and currents. These can either be directly measured, or simulated from a circuit design that consists of a set of models for all the constitutive components. The other independent data, that is, the higher-order time derivatives, are then calculated. In order to collect the data, the device under consideration is typically excited by a single-tone RF signal. The response of the device is characterised by the corresponding time-dependent terminal voltages and currents. In order to cover the state space of interest, a set of single-tone measurements (or simulations) at several incident powers and DC operating conditions is required. In the next section, we investigate how this procedure could be replaced by multisine excitations.

III. Use Of Multisine Excitations

To better approximate modulated excitation, we use multisine excitation in this work, in which the offset frequency between the tones is very small (kilohertz range) with respect to the RF frequency (gigahertz range). Use of the steady-state time-domain representation for model building can involve very cumbersome data processing, since one IF or envelope period would require several thousands of high-frequency periods and hence a multiple of this in number of data points, in order to meet the Nyquist criterion. For example, an IF period of 1/25 kHz or 40 μs encompasses 40,000 RF periods of 1 ns (considering 1 GHz as the fundamental frequency), resulting in at least 800,000 data points when 10 RF harmonics are being considered. The question is whether it is necessary to deal with all these data points, or can we sample this more efficiently.

One solution to this problem is use of the envelope formulation. Instead of having a phasor representation for each of the tones, we can summarize the behaviour using the fact that the amplitude and phase of the RF carrier (and its harmonics) vary as a function of time, or in case of $I_2(t)$ for example:

$$I_2(t) = \mathrm{Re}\{A_1(t)\exp(j\omega t + P_1(t)) + A_2(t)\exp(j2\omega t + P_2(t)) + \cdots + A_h(t)\exp(jh\omega t + P_h(t))\}, \quad (3)$$

with $A_i(t)$ and $P_i(t)$ representing the amplitude and the phase of the ith RF harmonic, h the number of RF harmonics considered, and ω the carrier frequency.
$A_i(t)$ and $P_i(t)$ vary slowly with respect to the RF time scale, and thus could be assumed constant locally around some time point t_{if} of the IF period. Equation (3) at around t_{if} becomes:

$$I_2(t)_{if} = \mathrm{Re}\{A_1(t_{if})\exp(j\omega t + P_1(t_{if})) + A_2(t_{if})\exp(j2\omega t + P_2(t_{if})) + \cdots + A_h(t_{if})\exp(jh\omega t + P_h(t_{if}))\}. \quad (4)$$

In other words, the instantaneous current at port 2 is now described by an RF spectrum by which the amplitudes and phases of the fundamental and its harmonics are essentially no longer time-dependent. Or, locally around t_{if}, we get the equivalent of one measurement (or simulation result) in the single-tone case, and consequently the earlier method, as described in Section II, can be applied. The result is that the data of one RF period are used to describe the device's behaviour over the coverage reached over this one RF period, which is a very small subset of the whole IF period. By 'sampling' the IF period, and by considering one RF period at each sample point, we get a collection of RF periods from which a 'joint' model can be built that will mimic well the device's behaviour across the state space covered by the multisine measurement. Concerning the sampling rate, or the number of RF periods considered, the Nyquist criterion (in terms of the IF period) can be used, in combination with considerations regarding a 'uniform' coverage of the state space [4]. For example, when considering 10 RF harmonics and 16 points along the IF period, the number of data points would be reduced from more than 800.000 (see example above) to 320. Even when using oversampling, this would drastically reduce the number of data points to be handled in the data processing.
Figure 1 shows the coverage of the (V_1, V_2) plane obtained after applying a 3-tone excitation to an amplifier. If the conventional time-domain representation is used, the numerous data points make up one big black spot (left figure). The reason is that a multisine is a collection of phasors that turn around at slightly different speeds (due to the small frequency offset), resulting in a large variation of instantaneous values. The right hand side of the figure shows how this space can be sampled efficiently. We consider 16 IF sampling points, and plot the corresponding RF trajectories. We can notice from this figure that this collection of trajectories covers well the (V_1, V_2) area of the 3-tone excitation. Note that a similar coverage could be obtained by 16 single-tone measurements (or simulations) with varying input powers. Therefore, an additional advantage of using a multi-tone excitation is that it can replace multiple single-tone experiments, which reduces the experiment time.

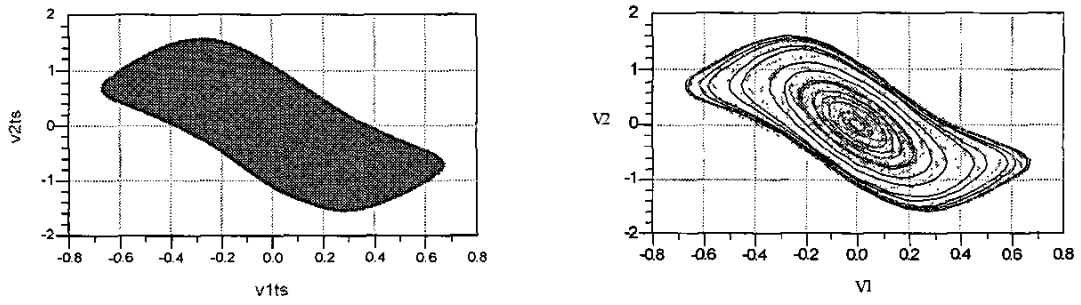

Figure 1: Left: Coverage of the (V_1, V_2) plane obtained by making use of one 3-tone excitation; right: the IF period is sampled equidistantly in time. At each of the 16 time instances considered, we consider one RF period. The 16 corresponding $V_2(t)$ trajectories as function of $V_1(t)$ are represented by the solid lines in the (V_1, V_2) plane. The purpose of the grey dots is just to indicate the (V_1, V_2) area as covered by the 3-tone excitation, which is identical to the (V_1, V_2) covered area on the left hand side plot.

In practice one has to check the error made when assuming that $A(t)$ and $P(t)$ are locally constant. Equation (4) implies that $I_2(t)_{if}$ is periodic, meaning that two subsequent RF periods should be identical. As an example, we excited an amplifier by a 65-tone signal. The RF frequency was 800 MHz and the offset between the tones was 25 kHz. Figure 2 represents two subsequent RF trajectories in the (V_1, V_2) plane. Marker m1 denotes the starting and end points of the trajectories. Were it periodic, the trajectories should be closed. The right-hand figure zooms in into the area around marker m1. Marker m2 denotes the starting point of trajectory 1, m3 the end of trajectory 1, and start of trajectory 2, and marker m4 shows the end point of trajectory 2. We notice that the RF trajectories are not closed, due to the varying $A(t)$ and $P(t)$, but that the error made is very small (below 0.3 mV). We should be aware however that this error depends strongly on the experimental conditions (device type, DC and RF operation conditions) and therefore should be checked systematically.

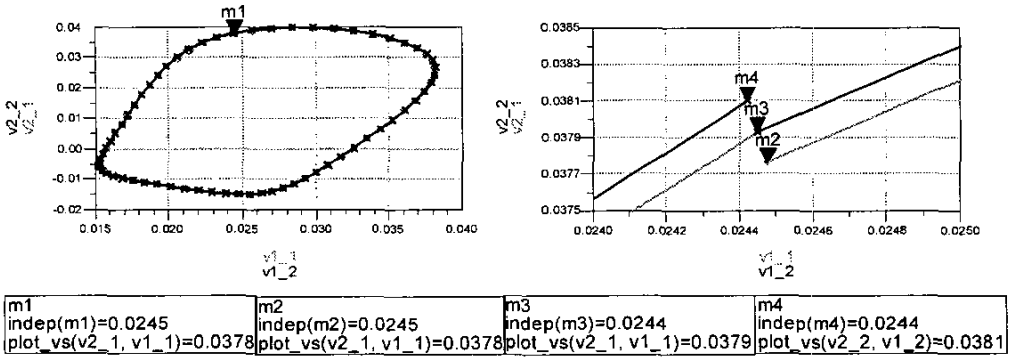

Figure 2: Two subsequent RF trajectories in the (V_1,V_2) plane. The grey solid line represents trajectory 1, and the black solid line trajectory 2.

Having these time-domain data, the modelling procedure can be continued. The number of required state variables can be estimated by use of techniques reported on earlier [4], and as the final step, the functions $f_1(.)$ and $f_2(.)$ can be determined. We have experienced that artificial neural networks (ANNs) are a good candidate to represent the functions $f_1(.)$ and $f_2(.)$ [7]. The reason is that the activation function can be selected such that the asymptotes of the model behave smoothly. This property is important for ensuring convergence in circuit simulators. For the ANN, we consider one hidden layer. The independent variables of equations (1) and (2) are the inputs, and the terminal currents are the outputs. The ANN is being trained using a back-propagation algorithm [8].
Results for two amplifiers are presented in the next Section.

IV. AMPLIFIER RESULTS

To demonstrate the validity of the proposed method, we constructed a model for two amplifiers. In the first case, the design of the amplifier is available in the RF circuit simulator. The model is consequently built starting with simulation results obtained from this design. The second case concerns a model based on actual large-signal measurements, performed on a packaged off-the-shelf amplifier. We verified beforehand that both amplifiers do not exhibit slow memory effects.

A. Model based on simulations

We consider an off-the-shelf RF amplifier whose design is available in our RF circuit simulator environment. The purpose of this study is to replace this design with a behavioural model. The

fundamental frequency is fixed at 800 MHz, and the excitation considered is a 3-tone signal with an offset of 25 kHz between the tones.

The first problem is to generate the necessary variables. The terminal currents and voltages are being simulated directly, but the (higher-order) time derivatives need to be calculated. This is straightforward in the conventional time-domain representation, but, again, it requires many data points. Therefore, we made use of the envelope analysis tool in the RF circuit simulator, as opposed to the harmonic-balance analysis tool, to determine these 'derived' variables.

The results obtained, after fitting an ANN, and implementing this ANN back into the RF circuit simulator, are represented by the following figures. Figure 3 compares b_2 as simulated by the original circuit design (left), and as simulated using the ANN (right). We notice that the 3 fundamental tones are very well predicted, as well as the intermodulation products down to a level of –30 dBm. To improve the prediction of the intermodulation products even further, a higher IF sampling rate should be used, such that the coverage obtained is better and the model is less susceptible to extrapolations and interpolations.

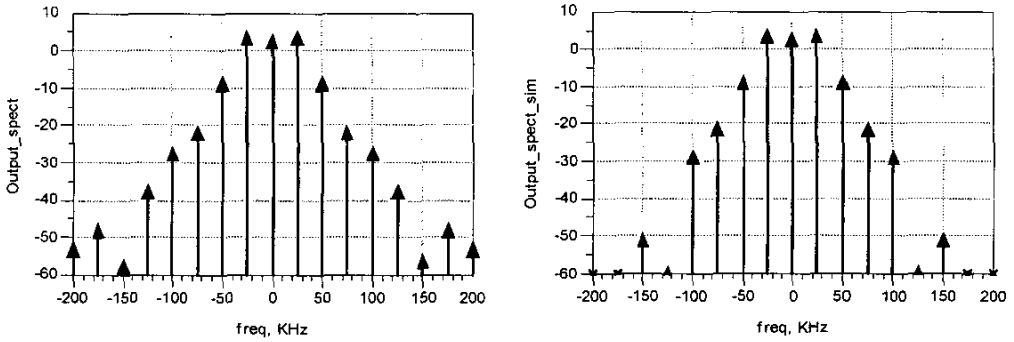

Figure 3: b_2 [in dBm] of the reference simulation (left) and as predicted by the ANN (right). The excitation is a 3-tone signal.

Next, it is important to evaluate how this model performs under excitation conditions, different from the ones present in the model generation process. Figure 4 compares b_2 as simulated by the original circuit design (left), and as simulated using the ANN (right), under a 5-tone excitation. Also, the accuracy is very good here.

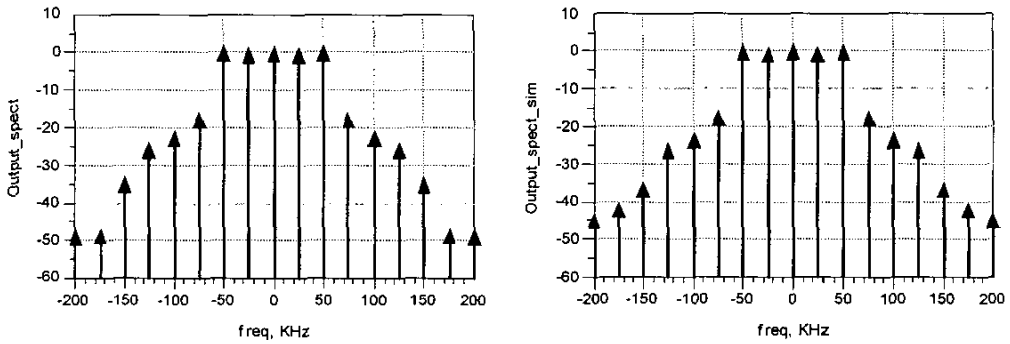

Figure 4: b_2 [in dBm] of the reference simulation (left) and as predicted by the ANN (right). The excitation is a 5-tone signal.

B. Model based on measurements

In this case, we characterised a packaged off-the-shelf amplifier (different from the one above) by means of a vectorial large-signal measurement system [9]. The fundamental frequency is 800 MHz and the multisine used is a 3-tone excitation, with an offset of 800 kHz. The terminal voltages and currents are measured, and the other independent variables are calculated from the measured quantities using envelope analysis. After training an ANN and implementing this in the RF circuit simulator, we obtain the results given by the following figures. Figure 5 compares the measured and simulated b_2 in the band near the carrier frequency of 800 MHz. Due to the large scale, we list separately the amplitude and phase values of both b_1 and b_2 at the three main frequencies in Tables 1 and 2. Figure 6 compares the measured and simulated b_2 at the second harmonic RF frequency. By way of comparison, we also present the simulation results of an ANN, built from power-swept single-tone measurements. From these figures and tables, we conclude that the 3-tone measurement-based model is accurate. The single-tone measurement-based model yields quite similar results, but it requires several (power-swept, and possibly also bias-swept) measurements, whereas one multisine based measurement is equivalent to several single-tone measurements, as explained in Section III.

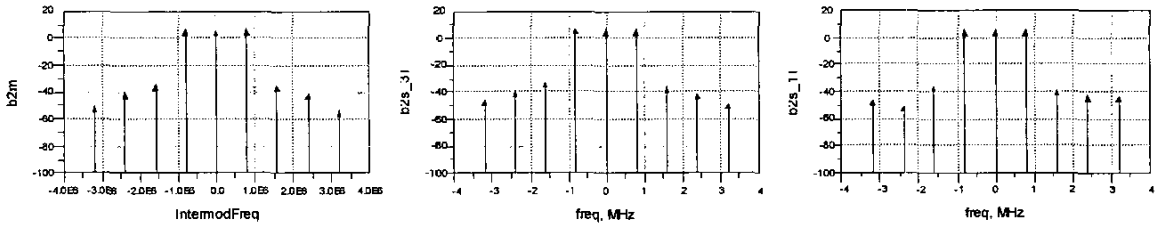

Figure 5: b_2 [in dBm] as measured (left), as predicted by the 3-tone measurement-based ANN (middle), and as predicted by the 1-tone measurement-based ANN (right). The excitation is a 3-tone signal.

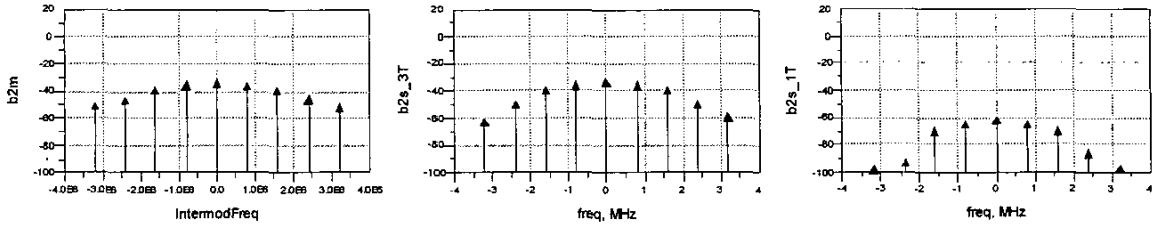

Figure 6: b_2 [in dBm] around the 2nd harmonic RF frequency, as measured (left), as predicted by the 3-tone measurement-based ANN (middle), and as predicted by the 1-tone measurement-based ANN (right). The excitation is a 3-tone signal.

	measured [dBm]	3T-model [dBm]	1T-model [dBm]	measured [°]	3T-model [°]	1T-model [°]
$b_{1,f0-\Delta f}$	-18.7	-18.7	-17.7	-85.0	-85.5	-83.9
$b_{1,f0}$	-19.0	-18.9	-17.8	30.1	30.3	33.4
$b_{1,f0+\Delta f}$	-18.8	-18.9	-18.0	146.4	146.8	152.0

Table 1: Comparison of the amplitude and phase of the measured, 3-tone measurement-based simulated, and 1-tone measurement-based simulated b_1 at the 3 main RF frequencies.

	measured [dBm]	3T-model [dBm]	1T-model [dBm]	measured [°]	3T-model [°]	1T-model [°]
$b_{2,f0-\Delta f}$	6.4	6.5	5.9	83.5	83.0	84.2
$b_{2,f0}$	6.1	6.1	5.7	-161.6	-161.7	-160.6
$b_{2,f0+\Delta f}$	6.3	6.2	5.9	-45.8	-45.3	-44.4

Table 2: Comparison of the amplitude and phase of the measured, 3-tone measurement-based simulated, and 1-tone measurement-based simulated b_2 at the 3 main RF frequencies.

Finally, as a better independent check, we evaluate the models' accuracy under a 65-tone excitation. Figure 7 compares the measured and simulated b_2 in the band near the carrier frequency of 800 MHz. Due to the large scale, we list separately the amplitude and phase values of both b_1 and b_2 at 3 selected frequencies in Tables 3 and 4. Again, we also present the simulation results of the 1-tone measurement-based ANN. These simulations were obtained using the harmonic-balance analysis tool. The second harmonic results are not shown for this case, because the harmonic level is very low (below –40 dBm). From this figure and tables, we can conclude that both the 1-tone and 3-tone measurement-based ANNs can predict well the 65-tone response. The 3-tone measurement-based ANN results are overall slightly better than those for the 1-tone measurement-based ANN.

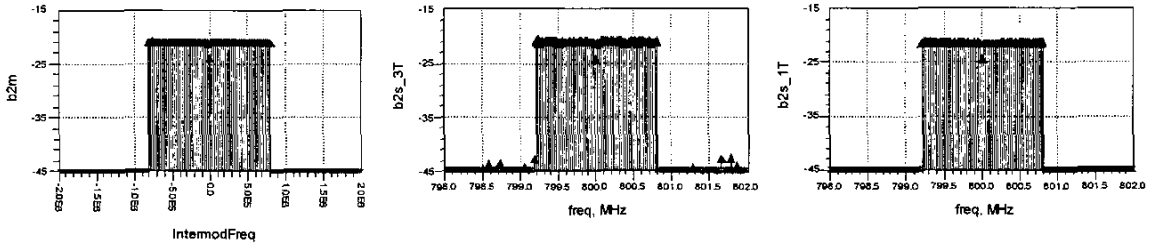

Figure 7: b_2 [in dBm] as measured (left), as predicted by the 3-tone measurement-based ANN (middle), and as predicted by the 1-tone measurement-based ANN (right). The excitation is a 65-tone signal.

	measured [dBm]	3T-model [dBm]	1T-model [dBm]	measured [°]	3T-model [°]	1T-model [°]
$b_{1,799.95MHz}$	-45.5	-45.5	-44.6	16.7	18.8	22.1
$b_{1,800.05MHz}$	-45.5	-45.7	-44.6	-53.0	-55.2	-48.6
$b_{1,800.1MHz}$	-45.6	-45.5	-44.7	-88.6	-87.6	-83.8

Table 3: Comparison of the amplitude and phase of the measured, 3-tone measurement-based simulated, and 1-tone measurement-based simulated b_1 at three selected frequencies.

	measured [dBm]	3T-model [dBm]	1T-model [dBm]	measured [°]	3T-model [°]	1T-model [°]
$b_{2,799.95MHz}$	-20.4	-20.5	-20.9	-173.9	-172.9	-173.0
$b_{2,800.05MHz}$	-20.4	-20.5	-20.9	115.6	112.3	117.0
$b_{2,800.1MHz}$	-20.5	-20.4	-20.9	79.5	80.8	80.4

Table 4: Comparison of the amplitude and phase of the measured, 3-tone measurement-based simulated, and 1-tone measurement-based simulated b_2 at three selected frequencies.

V. CONCLUSIONS

We have shown that multi-tone excitations are beneficial for RF behavioural modelling, as they can significantly reduce the number of experiments needed for data collection. Moreover, in case of devices that exhibit no low-frequency memory effects, the data handling can be reduced drastically by 'sampling' or subdividing the IF period in a number of RF periods that can be independently treated. Finally, we demonstrated the proposed method by constructing accurate models from both amplifier design simulation results and from vectorial large-signal amplifier measurements.

ACKNOWLEDGEMENTS

D. Schreurs is supported by the Fund for Scientific Research-Flanders as a post-doctoral fellow. Division ESAT-TELEMIC of the K.U.Leuven acknowledges Agilent Technologies for the donation of the NNMS.

REFERENCES

[1] T. Wang and T. Brazil, "The estimation of Volterra transfer functions with applications to RF power amplifier behavior evaluation for CDMA digital communication", IEEE International Microwave Symposium, pp. 425-428, 2000.

[2] H. Ku, M. McKinley, and J. Kenney, "Extraction of accurate behavioral models for power amplifiers with memory effects using two-tone measurements", IEEE International Microwave Symposium, pp. 139-142, 2002.

[3] T. Reveyrand, C. Maziere, J.-M. Nebus, R. Quere, A. Mallet, L. Lapierre, and J. Sombrin, "A calibrated time domain envelope measurement system for the behavioral modeling of power amplifiers", Gallium Arsenide Application Symposium, pp. 237-240, 2002.

[4] D. Schreurs, J. Wood, N. Tufillaro, L. Barford, and D. E. Root, "Construction of behavioural models for microwave devices from time-domain large-signal measurements to speed-up high-level design simulations", International Journal of RF and Microwave Computer Aided Engineering, Vol. 13, No. 1, pp. 54-61, 2003.

[5] K. A. Remley, "Multisine excitation for ACPR measurements", IEEE International Microwave Symposium, 4 p., June 2003.

[6] M. Kennel, R. Brown, and H. Abarbanel, "Determining embedding dimension for phase-space reconstruction using a geometrical construction", Phys. Rev. A, Vol. 45, pp. 3403-3411, 1992.

[7] D. Schreurs, J. Jargon, K. Remley, D. DeGroot, and K.C. Gupta, "ANN model for HEMTs constructed from large-signal time-domain measurements", Automatic RF Techniques Group Conference (ARFTG), 6 p., June 2002.

[8] V. Devabhaktuni, M. Yagoub, and Q.-J. Zhang, "A robust algorithm for automatic development of neural-network models for microwave applications", IEEE Trans. Microwave Theory and Techniques, Vol. 49, No. 12, pp. 2282-2291, 2001.

[9] J. Verspecht, P. Debie, A. Barel, and L. Martens, "Accurate on wafer measurement of phase and amplitude of the spectral components of incident and scattered voltage waves at the signal ports of a nonlinear microwave device", IEEE International Microwave Symposium, pp. 1029-1032, 1995.